A&A manuscript no.
(will be inserted by hand later)

Your thesaurus codes are:
05 (09.03.1; 09.04.1; 13.07.1)

Dust and dark Gamma-Ray Bursts: mutual implications

S.D. Vergani[1], E. Molinari[1], F.M. Zerbi[1] and G.Chincarini[2,]

[1] INAF-Osservatorio Astronomico di Brera, Via Bianchi 46 I-23807 Merate (Lc) Italy

[2] Università di Milano Bicocca

email: vergani@merate.mi.astro.it

the date of receipt and acceptance should be inserted later

Abstract. In a cosmological context dust has been always poorly understood. That is true also for the statistic of Gamma-Ray Bursts (GRBs) so that we started a program to understand its role both in relation to GRBs and in function of z.

This paper presents a composite model in this direction. The model considers a rather generic distribution of dust in a spiral galaxy and considers the effect of changing some of the parameters characterizing the dust grains, size in particular. We first simulated 500 GRBs distributed as the host galaxy mass distribution, using as model the Milky Way. If we consider dust with the same properties as that we observe in the Milky Way, we find that due to absorption we miss $\sim 10\%$ of the afterglows assuming we observe the event within about 1 hour or even within 100s.

In our second set of simulations we placed GRBs randomly inside giants molecular clouds, considering different kinds of dust inside and outside the host cloud and the effect of dust sublimation caused by the GRB inside the clouds. In this case absorption is mainly due to the host cloud and the physical properties of dust play a strong role. Computations from this model agree with the hypothesis of host galaxies with extinction curve similar to that of the Small Magellanic Cloud, whereas the host cloud could be also characterized by dust with larger grains. Unfortunately, the present statistics lack solid grounds, being based on hardly compatible observations, at different time from the burst and with different limiting magnitudes. To confirm our findings we need a set of homogeneous infrared observations. The use of coming dedicated infrared telescopes, like REM, will provide a wealth of cases of new afterglow observations.

Key words: dark Gamma-Ray burst – dust – ISM

Send offprint requests to: S.D. Vergani

Table 1. Physical characteristics of H_2 galactic clouds.

(1)	(2)	(3)	(4)	(5)	(6)	(7)
	R	n_H	No.(bulge)	No.(disk)	Unit mass	Total mass
GMC	20	$5 \cdot 10^2$	800	4000	$4 \cdot 10^5$	$1.92 \cdot 10^9$
DC	2	$5 \cdot 10^4$	16000	80000	$5 \cdot 10^3$	$4.8 \cdot 10^8$

Radius is in pc and n_H in cm^{-3}. Masses are in $M_\odot$.

1. Introduction

The observations show that about 50% of the detected GRBs are not visible at optical wavelengths. Statistics refers to well localized bursts (Bloom, Kulkarni & Djorgovski 2002) with an X ray flux rather similar to those that have been detected also in the optical band. The rapid decline of the optical afterglow (Fynbo et al. 2002, Berger et al. 2002) can not explain the observations as well and that is why we call them dark bursts and an explanation has yet to be found.

In two cases, GRB 970828 and GRB 990506, in spite of lacking the optical afterglow we were able to identify the host galaxies (z=0.958 and z= 1.3 respectively) so that in these cases it is evident that high redshift is not the cause of the optical flux extinction. A possible explanation is that the events have been obscured by dust. After the first part of our work was completed (Vergani 2002) Reichart (2001) and Reichart & Price (2002) made a case for a strong absorption occurring in the molecular clouds where the event originates. This is in agreement with the current thinking that GRBs are related to massive star formation which is strongly correlated with very dusty regions. Whether we are dealing with a particular type of galaxies is not known. Ramirez-Ruiz, Threntham & Blain 2002 assert that we might be dealing with ULIRG (Ultra Luminous Infrared Galaxies) or alike objects and that the extinction is essentially due to the dust distribution present in these galaxies. We do not have observational evidence that this is the case however. No matter how the dust is at work, we must also account for the local process of dust sublimation and understand how much dust a burst is capable of sublimating and sweeping out.

We decided to tackle the problem first theoretically, and this paper report part of our work in this direction, and observationally by building the robotic NIR Telescope REM (Zerbi et al. 2002, Chincarini et al. 2003). The statistics of GRBs will also largely increase as soon as the Swift satellite will be launched (Gehrels et al. 2003).

In section 2 we discuss how we model the dust itself, Section 3 is devoted to the construction of the simple host galaxy; a basic GRB distribution models and results are

presented in section 4. In section 5 and 6 we associate GRBs with giant molecular clouds and we explore its implications. Conclusions are drawn in section 7.

2. Dust model

The afterglow radiation reaches the observer after interacting with circunburst material, host ISM, IGM and the ISM of our galaxy. In this work we consider only the interaction with the dust in the ISM of the host galaxy.

Our dust model is based on Mathis, Rumpl & Nordsiek (1977) model, improved by Mathis (1986). We suppose that dust is made by spherical grains composed by 50% of graphite and 50% of silicates with a grain size a distributed as

$$n(a) = n_0 a^{-3.5} \tag{1}$$

with $a_{min} = 0.005\mu$m, $a_{max} = 0.25\mu$m and n_0, proportional to the neutral hydrogen density ($n_H[\mathrm{cm}^{-3}]$), used by Venemans & Blain 2001.

The variation in magnitudes produced on flux after interacting with dust grains is

$$\Delta m \propto \int_0^\infty Q_{ext} \pi a^2 n(a) da \tag{2}$$

with Q_{ext} =extinction efficiency (sum of scattering and absorption efficiency, see Van de Hulst 1957).

By varying in our model the fraction of the two types of materials, the exponent of the grain size distribution and the grain size, the result is a change in the scale of the curve without modifying its shape. We cannot therefore disentangle their contribution from different amounts of hydrogen column densities (NH[cm^{-2}]) along the line of sight. On the contrary the size of the grains play a strong role. Large grains, which could be present in regions with intense star formation (Maiolino, Marconi & Oliva 2001) or in circunburst environment after the burst has sublimated the smaller grains (Venemans & Blain), cause the extinction curve to flatten. For dust composed only by large grains ($a_{min} = 1\mu$m, $a_{max} = 2\mu$m) our computations predict a fixed value of $\Delta m \sim 0.1$, in agreement with the theory, that predict for the case $2a > \lambda$ a fixed value of $Q_{ext} \sim 2$ (Fig. 1). The effects of modifying a_{min} with fixed a_{max} are not relevant.

3. Galactic-like model

We model an host galaxy similar to our Milky Way, where the dust is distributed as the neutral hydrogen, both molecular (H_2) and atomic (HI).

For the galactic hydrogen surface density we adopt the values taken from Scoville (1992), and Binney & Merrifield (1998).

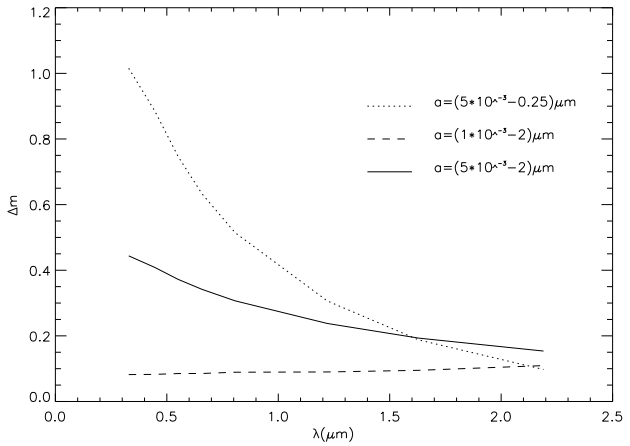

Fig. 1. Extinction curves produced by varying the dust grain size in case of an hydrogen column density of $10^{21} cm^{-2}$. Dotted steeper curve represents the extinction considering our Galactic-like dust model (STD, see Tab. 4) based on Mathis (1986). Dashed and solid lines describe the extinction curve in case of a dust composed by larger grains (OLG and LRG, respectively).

For H_2, two gaussian fits were drawn on nuclear and disk data: namely the gas density has been expressed as:

$$\mathrm{NH(bulge)} \propto e^{\frac{-R^2}{2(0.28)^2}} \mathrm{cm}^{-2} \tag{3}$$

and

$$\mathrm{NH(disk)} \propto e^{\frac{-(R-5.03)^2}{2(1.8)^2}} \mathrm{cm}^{-2} \tag{4}$$

for the bulge and the disk, where R is the radial distance in cylindrical coordinates (kpc). The total mass of galactic H_2 is distributed with $4 \cdot 10^8 M\odot$ in the bulge and $2 \cdot 10^9 M\odot$ in the disk. The H_2 clouds are present in two distinct morphologies, which we catalogue as giant molecular clouds (GMC) and dense clouds (DC) whose adopted characteristics are summarized in Table 1. An algorithm assigns positions, with a random distribution weighted by Galaxy mass density, to GMC and DC.

Neutral atomic hydrogen is present in a diffuse form throughout the disk system with a total mass of $4.3 \cdot 10^9 \odot$. Following Binney & Merrifield (1998), we simplify its distribution as being sharply confined in the radial interval $3 < R < 18$ (R in kpc) with a spatial density represented by $n_H[\mathrm{cm}^{-3}] = 0.797 e^{-h^2/0.02}$ (where h is the height from Galactic plane in kpc). In Fig. 2 we plot the adopted fits for HI (dashed line) and H_2 (solid lines) surface densities, while Fig. 3 shows the appearance of the host galaxy hydrogen distribution .

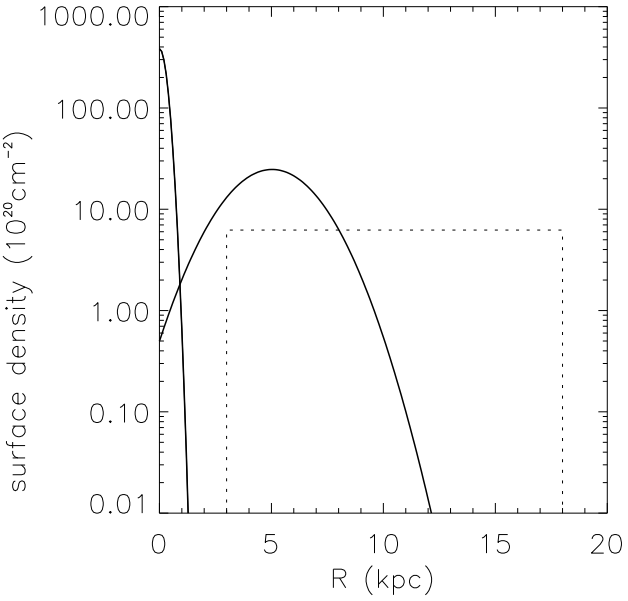

Fig. 2. Milky Way hydrogen column density as a function of radial distance R in kpc. The two solid curves are the two gaussian fits to the distribution reported in Scoville (1992), for the molecular hydrogen (H_2). Dashed line is the atomic hydrogen (HI) surface density, simplified as a box function between 3 and 18 kpc from galactic center.

4. Basic GRBs absorption model

We suppose that the GRBs are distributed as the luminosity (barionic mass) of the host Milky Way-like galaxy. Using the Milky Way photometric model of Kent, Dame & Fazio (1991), we have

$$j_d(R,h) = \frac{I_d}{2h_0} e^{-R/R_d - |h|/h_0}, \tag{5}$$

with

$$h_0 = \left[0.165 + 0.21(R/R_0 - \frac{5}{8})\right] \text{ kpc}, \tag{6}$$

R_d =3kpc, R_0 =8kpc and the central surface brightness I_d =1000 $L_\odot pc^{-2}$.

The bulge has been modeled using a King profile

$$I(r) \propto [1 + (r/r_c)^2]^{-3/2} \tag{7}$$

with r_c =0.25kpc.

The fraction of GRBs located in the Galactic disk and in the bulge is derived assuming a mass ratio disk to bulge of 4.5.

The burst occurs randomly using as weighting function the distribution of mass of the galactic model. The observer is located randomly over a 4π solid angle.

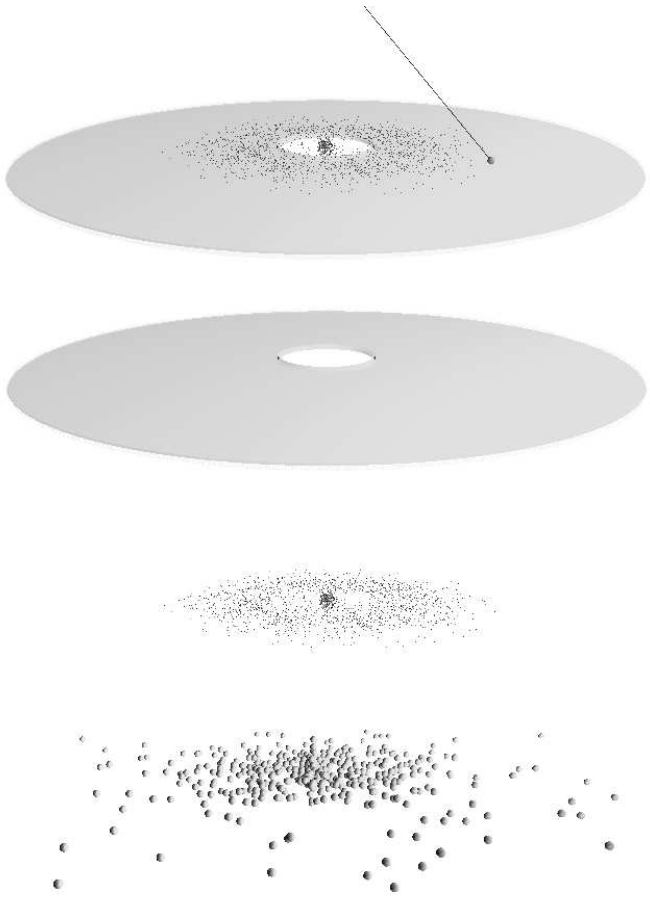

Fig. 3. A rendered image of our host galaxy model. The top figure is the complete model with the sphere on the right which represents a randomly positioned GRB. Its line of sight crosses the galactic plane. Below the distribution of the atomic hydrogen (HI) and H_2 clouds (both GMC and DC) are separately shown. In the bottom picture the simulated distribution of the 500 GRBs.

Each molecular hydrogen cloud is accounted for absorption and the amount of NH is integrated along the line of sight. The quantized NH amount is then $4.5 \cdot 10^{22}\mathrm{cm}^{-2}$ for the GMC and $2.25 \cdot 10^{23}\mathrm{cm}^{-2}$ for the DC.

The atomic diffuse hydrogen is summed integrating along the line of sight from the GRB to a radius of 20 kpc from the galactic center. The HI contribution ranges therefore from a null value to $7 \cdot 10^{22}\mathrm{cm}^{-2}$, with a pick at about $5 \cdot 10^{20}\mathrm{cm}^{-2}$ not sufficient to obscure the afterglow. On the other hand the encounter of a single cloud yields values of NH of about $5 \cdot 10^{22}\mathrm{cm}^{-2}$ (GMC) or $5 \cdot 10^{23}\mathrm{cm}^{-2}$ (DC) largely enough to completely absorb the optical afterglow.

The total amount of NH is computed and catalogued for the whole 500 GRBs set and for the subset of 91 nuclear bursts. In Fig. 4 the histogram of the total NH distribu-

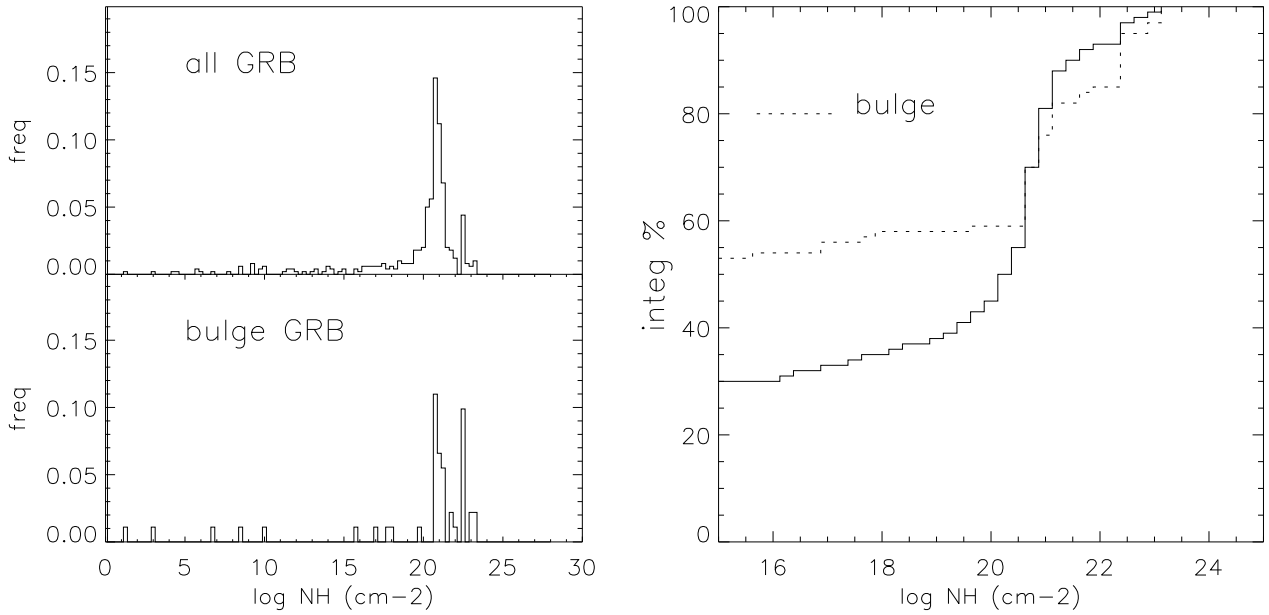

Fig. 4. Hydrogen column density distribution for 500 simulated GRBs.

Table 2. Extinction limits computed on the basis of the limiting magnitudes of different instruments and of GRB990123 afterglow light curve. NH values are computed using the dust model in Section 2.

(1)	(2)	(3)	(4)	(5)	(6)	(7)	(8)	(9)	(10)
	sec	m_R	m_K	$R_{\rm lim}$	$K_{\rm lim}$	A_R	A_K	NH_R	NH_K
prompt	100	10	7.5	19	15.5	9	8	0.86	2.13
late	5000	16	13.5	24	20.5	8	7	0.76	1.87

(3)(4) In these columns are reported light curve values GRB990123-like.

(5)(6) Prompt observation simulated with REM (Vergani 2002, Table 2.3), late observation simulated with ISAAC and FORS (see http://www.eso.org/oserving/etc/ for its ETC time estimates)

(9)(10) in units of $10^{22}{\rm cm}^{-2}$

tion is shown for the two populations. To better appreciate the difference a cumulative distribution for a smaller range of column densities is reported aside.

The amount of dark GRBs due to dust absorption can now be estimated, once we have fixed the limiting magnitude of our telescopes in the various passbands and the typical apparent magnitude of GRB afterglows. We associate randomly to each GRB a jet opening angle θ following the law $\propto \theta^{-0.85}$ that we have extrapolated from the known jet angles reported by Bloom, Frail & Kulkarni (2003) (see Fig.7, upper panel). Note

Table 3. Optical (R) and infrared (K) transient loss (%). Prompt and late observation cases are reported for z=1 galaxy position.

(1)	(2)	(3)	(4)	(5)
	% lost of all GRBs		% lost of bulge GRBs	
	R	K	R	K
z=1 prompt	9	7	18	14
late	9	7	18	14

that the θ distribution is truncated as $0.05 < \theta[rad] < 0.6$. Considering the luminosity L proportional to θ^{-2}, we calculate the magnitudes R and K of GRBs at 100s and 5000s, taking as reference GRB990123 shifted at z=1 (that is the observed mean redshift of GRBs, Hurley et al. 2002), the color data by Simon et al. (2001) and using the relation

$$m_{GRB} = m_{990123} + 5\log(\theta/\theta_{990123}) \quad (8)$$

where θ_{990123} and m_{990123} are the jet angle and the magnitudes of GRB990123. To compute the limiting magnitudes we assume to use REM telescope for the fast response to the GRB alert in R and K bands, FORS and ISAAC camera of ESO/VLT for the long term observations (Tab. 2).

For each GRB we calculate the extinction in R and K caused by the traversed NH column density. We are then able to compute the percentage of lost afterglows due to dust absorption under the assumption that the host galaxy at z=1 has dust properties similar to Milky Way.

In Table 2 R and K magnitudes of prompt and late observations for GRB990123-like events are reported. The values of NH quoted in columns (9) and (10) represent the computed amount of NH needed, according to our dust model, to obtain the extinction values of column (7) and (8). The summary of Table 3 is a clear indication that only a relatively small fraction of GRBs is *not* observed due to dust extinction in the case of a host galaxy at z=1.

5. GRBs in molecular clouds

Our results show that, if the GRBs distribution is similar to the mass distribution and if the dust of the host galaxies has the same characteristic of Galactic dust, the percentage of dark GRBs due to dust obscuring is rather low. There is no relevant difference between R and K observations and between percentages relatives to observations taken at 100s and 5000s. It also happens that no burst, out of the 500 considered, occurs statistically

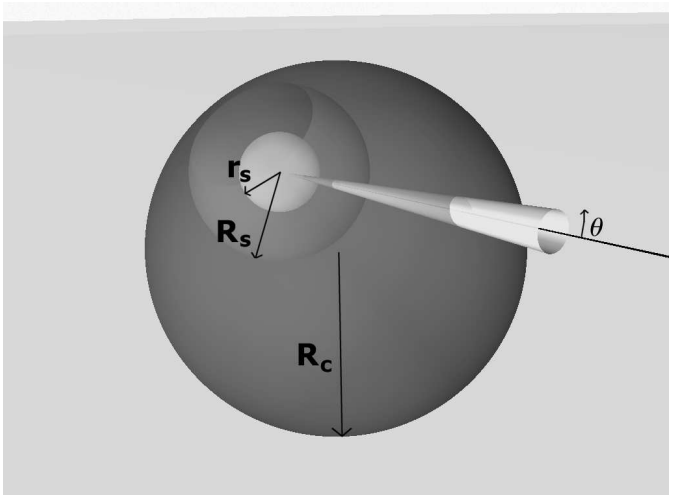

Fig. 5. Geometry around the GRB location explaining the shapes of the four regions whose content in terms of dust is parameterized in our models. The regions are spherical shells centered on the GRB location delimited by r_s(the radius up to which all dust grains are destroyed), R_s(the radius up to which grains with radius smaller 1μm are destroyed), R_C (the radius of the giant molecular cloud) and the border of the galaxy. θ is the jet opening angle associated to the GRB event.

inside a molecular cloud. In this scenario the majority of dark bursts could be due to high redshift Ly-α absorption.

We then consider the case that GRBs follow the distribution of giant molecular clouds. Physically the assumption is that of a strong connection between GRBs and massive stars formation.

Within this framework, we place 5000 GRBs inside our modeled giant molecular clouds, that have similar characteristics respect the supposed typical GMC GRBs host described by Galama & Wijers (2001).

The first aspect to consider is dust sublimation by the optical-UV flash accompanying the GRB, phenomenon likely confirmed by the observations of the afterglow light curve of GRB 990123 (Akerlof et al. 1999). We consider the results of Waxman & Draine (2000) and Reichart 2001b that compute the radius up to which the dust is sublimated, which is also a function of dust grain size. In case of a canonical distribution of graphite and silicate grain size, the sublimation radius is $R_s \simeq 10 L_{49}^{1/2} pc$ where L_{49} is the 1-7.5eV (1600-12000Å) isotropic-equivalent peak luminosity of the optical flash in unit of $10^{49} ergs^{-1}$, that is the 1-7.5eV isotropic-equivalent peak luminosity of the optical flash of GRB990123.

Inside the host cloud we consider both the case of a standard galactic dust and the case of a dust, already present before the sublimation took place, with larger grain size with $a_{min} = 0.005\mu$m, $a_{max} = 2\mu$m, because the connection of GRBs and intense star

formation regions (Galama & Wijers (2001)), as described in §2. Moreover, in the case of large grains, we have to consider two different sublimation radius: an inner one (r_s) up to which all grain are destroyed and a larger one (R_s) up to which only the grains whit radius smaller than 1μm can be sublimated (Venemans & Blain).

R_s and r_s vary with the intensity of the peak luminosity of the optical flash, that we can suppose depending on the GRB jet opening angle θ. We calculate for each GRB R_s and r_s as $R_s = R_{s990123} * \theta_{990123}/\theta$ and $r_s = r_{s990123} * \theta_{990123}/\theta$, where $R_{s990123}$, $r_{s990123}$ and θ_{990123} are the two sublimation radius and the jet opening angle of GRB990123.

To each of the 5000 simulated GRBs is associated a random line of sight passing through 4 regions: $\Re$1 is the inner region from the GRB to r_s (the radius up to which all dust grains are destroyed); $\Re$2 goes from r_s to R_s, where large grains (radii from 1μm to 2 μm) are allowed to survive; $\Re$3 is the rest on undisturbed host cloud dust; $\Re$4 is the host galaxy outside the host cloud, consisting of all other molecular clouds and of the diffuse medium (see Fig.5). In these regions we place 5 kind of dust yielding ten different models.

In the first three models, to calculate the extinction in the region outside the host molecular clouds, we use our Galactic-like dust model. In $\Re$3, that is the part inside the host molecular clouds where there is no sublimation, 2 scenarios are explored: standard galactic dust (model 2 and 3) or a similar one but with larger grains ($a_{max} = 2\mu$m, model 1). Moreover, in model 2 we suppose that dust in the whole cloud is standard and thus sublimated both in $\Re$1 and $\Re$2, whereas in model 1 and 3 the circunburst medium is supposed to be characterized by dust with $a_{max} = 2\mu$m, thus in $\Re$2 dust grains larger than 1μm are left.

Hyorth et al., 2003 have recently supported the hypothesis that GRBs environment has an extinction curve similar to the one of Small Magellanic Cloud (SMC), so, in model 1smc, 2smc and 3smc we present the same scenario of model 1, 2 and n 3 but considering SMC extinction inside the cloud and/or in the host galaxy. Both the cases of extinction caused by larger grains or SMC-like dust agree with the non detection of the $\lambda = 2175\mathring{A}$ bump (Galama & Wijers (2001)), that is instead a significant feature of Galactic-like dust.

Simulations by Perna et al. 2003, show that if we consider dust with properties similar to the Galactic one, burst energy sublimes very quickly silicate grains present in the circunburst medium differently from graphite made grain that need a longer time to be destroyed and whose sublimation is more efficient on the smaller grains. On this basis, we think reasonable to consider models (model 1b, 3b, 1smcb and 3smcb) in which dust in $\Re$2 region is composed only by graphite grain with $a_{min} = 1\mu$m, $a_{max} = 2\mu$m. Table 4 shows all the cases.

Table 4. Regions around GRB location and their contents in term of dust type as adopted in our computations. Dust model used are: STD (our model of standard Galactic dust, with grain radii from 0.005μm to 0.25μm); LRG (with added larger grains, from 0.005μm to 2μm); OLG (only large grains, left from partial sublimation, with radii from 1μm to 2μm); GRA (only large graphite grains, left from partial sublimation) SMC (dust with low extinction similar to Small Magellanic Clouds); SUB (no dust, completely sublimated by the burst).

(1)	(2)	(3)	(4)	(5)
	$\Re 1$	$\Re 2$	$\Re 3$	$\Re 4$
model 1	SUB	OLG	LRG	STD
model 1b	SUB	GRA	LRG	STD
model 2	SUB	SUB	STD	STD
model 3	SUB	OLG	STD	STD
model 3b	SUB	GRA	LRG	STD
model 1smc	SUB	OLG	LRG	SMC
model 1smcb	SUB	GRA	LRG	SMC
model 2smc	SUB	SUB	SMC	SMC
model 3smc	SUB	OLG	SMC	SMC
model 3smcb	SUB	GRA	SMC	SMC

6. Results

The percentage of dust obscured afterglows for each model is computed summing all the absorption intervening in the four regions. Critical limiting magnitudes, beyond which the transient is no more visible, are taken from columns (5) and (6) of Tab. 2 while extinction curves used for standard Galactic dust and larger grain dust are respectively the dotted and the solid ones represented in Fig. 1. For SMC extinction curve we use the one reported by Weingartner & Draine (2001).

If in $\Re 2$ there are only grains larger than 2μm (both in case of standard and graphite only grains) we use dashed curve of Fig. 1, but multiplied respectively by a factor $F_1 = \int_1^2 a^{-0.5} da / \int_{0.005}^2 a^{-0.5} da$ and $F_2 = 0.5 * F_1$ taking into account that total dust mass is decreased. The 0.5 factor takes into account that half of the dust population (silicates) has completely disappeared.

In Tab. 5 results for different models are reported. It is evident that content in $\Re 2$ is almost not significant, whereas most of the extinction take place in $\Re 3$, so the content of this region has a determinant role. In Fig. 6 we plot percentages for relevant cases.

Table 5. Optical (R) and infrared (K) transient loss (%) in the GRB-GMC association scenario. The models are described in text and Tab. 4.

(1)	(2)	(3)	(4)	(5)
	R		K	
	prompt	late	prompt	late
model 1	53.0	57.3	38.8	44.8
model 1b	52.8	57.1	38.5	44.5
model 2	67.9	69.8	49.5	54.0
model 3	68.2	70.0	49.9	54.5
model 3b	57.8	57.1	38.5	44.5
model 1smc	46.8	51.1	29.9	36.6
model 1smcb	46.6	50.8	29.4	36.4
model 2smc	7.0	10.4	0.2	0.3
model 3smc	7.2	10.7	0.2	0.4
model 3smcb	7.1	10.6	0.2	0.3

In the lower panels of Fig. 7, we show magnitudes distributions (R and K) of the simulated afterglows after 100s for GRBs at z=1. Together with the complete population, the distributions of observed transient for the different models are plotted.

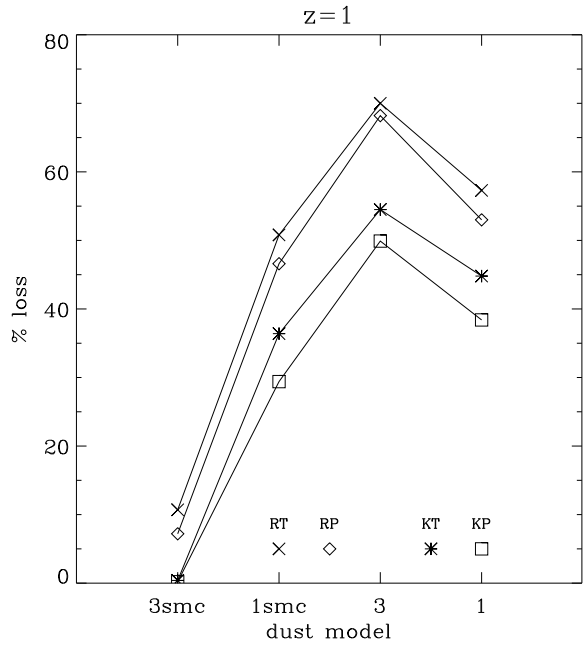

Fig. 6. Trends for the most relevant models of the percentage for prompt (RP, KP) and late (RT, KT) observations in R and K bands of dark bursts caused by dust extinction.

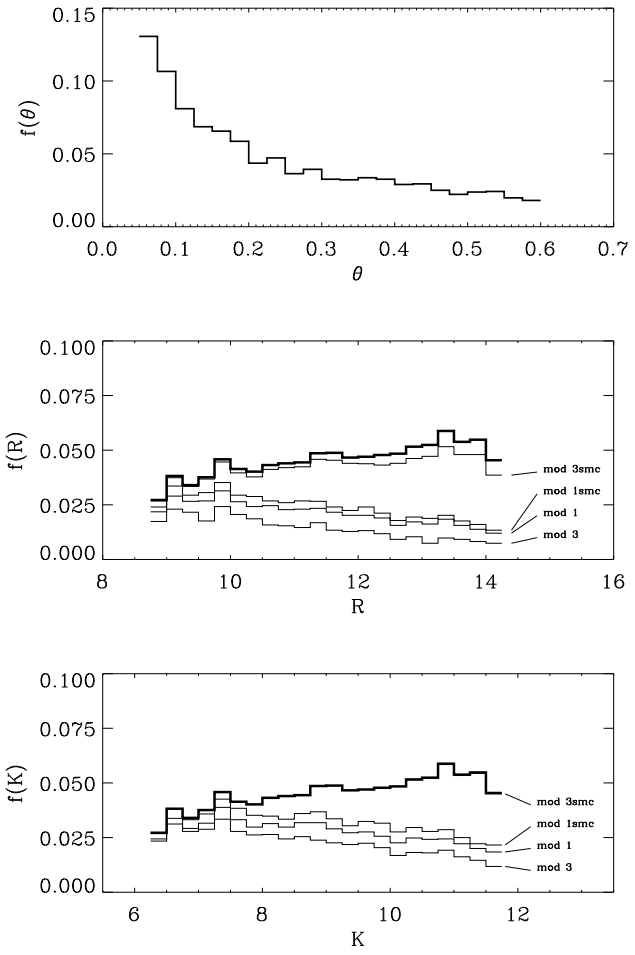

Fig. 7. Distribution of the θ jet opening angles of our 5000 GRBs simulated sample (upper panel). The parent distribution follows a $\theta^{-0.85}$ law after a fit to observed jet angles. The middle panel shows the translation of jet angles in R magnitudes (heavy line). The transformation lays on the zero point of a GRB990123-like event at z=1 ($\theta = 0.086$, R=10, K=7.5) and the assumption of the conservation of the total flux on the emitting solid angle ($\propto \theta^2$). Thinner lines are the luminosity function of the promptly observed (non absorbed in our simulations) afterglows in the R band. The four histograms refer to different models: 1, 3, 1smc and 3smc. In the lower panel the same set of distributions are plotted for the K filter (note that model 3smc does not differ from the original distribution, plotted as a heavy line).

A comparison of our simulation thought in view of Swift and REM with observational data available now would be misleading. From our point of view it is practically impossible to extract a statistically significant number (e.g. % of real dark bursts) from a set of observations performed with different telescopes (i.e. limiting magnitudes) and at different time from the burst. To stress this point we compute at different times the per-

centage of events for which the OT would not be observed even without dust extinction, considering the light curves of our simulated GRBs and fixing R limiting magnitude of $R_{lim} = 20.5$. Solid bold line in Fig. 8 shows that for the majority of data observational times the percentage of lost events is significant. Dashed bold line of Fig. 8 reports the computation made for the K infrared transient with $K'_{lim} = 19$.

Recently Klose et al. (2003) have dealt with a GRB (GRB020819) whose afterglow has been searched without success in K', 0.37 days after the burst down to K'=19 and in R band 0.13 days after the burst down to R=20.5. We report these observational times and magnitudes in Fig. 8: we notice that we can not exclude that GRB020819 could not be a real obscured or high redshift burst. It is also worth noting that our computations remark that if the observations reach $R_{lim} = 24$, the value at 0.13 days of the R band curve not affected by dust is null and that late K observations (more than 6 hours after the burst) are always sensibly biased.

We add to Fig. 8 the R band results of our models (i.e. considering extinction) at the same magnitude limit.

7. Conclusions

We have considered different kinds of dust and their role in obscuring optical and NIR afterglows of GRBs simulated with different distributions inside a galaxy at z=1. In the case of GRBs occurring inside giant molecular clouds, our simulations show that dust in GRBs host galaxies has not the same properties of galactic dust, otherwise dark GRBs would be more than observational data say. Furthermore our results agree with the hypothesis of dust extinction curve of GRBs host galaxies similar to that of SMC. Moreover, if the host molecular cloud is characterized by large dust grains, high redshift plays a minimal role in the causes of dark GRBs. The opposite situation takes place if also inside the host molecular cloud dust has SMC properties.

Once we will gather enough prompt K observations we will be able to estimate the nature of dust present in host molecular clouds from the fraction of lost K afterglows.

We underline the fact that with present observational data it is impossible to produce a real statistic for dark bursts due to the late and varying time of observations and to the different magnitudes reached.

In the future, from the afterglow results given by Swift and REM, we will be able to determine the nature of dark GRBs. Indeed with a further refinement of the model and a good statistics of bursts observed in various colors we will certainly be able to know which kind of dust is present in the environment of the burst.

Acknowledgements. The authors want to thank Stefano Covino and Daniele Malesani for the useful discussions.

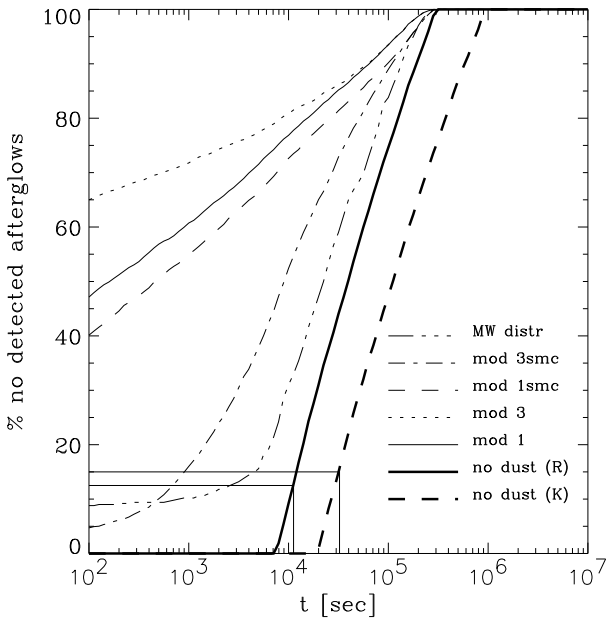

Fig. 8. Percentage of lost afterglows in function of observing time for GRB at z=1 with our simulated light curves. Solid bold line represents the R band curve without considering dust extinction, $R_{lim} = 21$; dashed bold line represents the K band curve without considering dust extinction, $K_{lim} = 19$, whereas the other curves report R band results from our models calculated for $R_{lim} = 21$. Two line intersections show the percentages in R and K relatives to the data of GRB020819.

References

Akerlof, C., Balsano, R., Barthelemy, S., et al. 1999, Nature, 398, 400

Berger, E., Kulkarni, S.R., Bloom, J.S., et al. 2002, Astrophys. J., 581, 981

Binney, J. & Merrifield, M. 1998, in Galactic Astronomy, ed. Princeton University Press, page 559, Fig.9.19

Bloom, J.S., Kulkarni, S.R. & Djorgovski, S.G. 2002, Astrophys. J., 123, 1111

Bloom, J.S., Frail, D.A. & Kulkarni, S.R. 2003, Astrophys. J., 594, 674

Chincarini, G., Zerbi, F.M., Antonelli, A. et al. 2003, ESO Messenger, in press

Fynbo, J.U., Jensen, B.L., Gorosabel, J., et al. 2002, Astron. Astrophys., 369, 373

Galama, T. & Wijers, R.A.M.J. 2001, Astrophys. J., 549, L209

Geherels, N., Swift Team 2002, AAS, 200, 3001

Hjorth, J., Moller, P., Gorosabel, J. et al. 2003, Astrophys. J., in press, astro-ph/0211620

Hurley, K., Sari, R. & Djorgovski, S.G. 2002, astro-ph/0211620

Kent, S.M., Dame, T.M. & Fazio, G. 1991, ApJ, 378, 131

Klose, S., Henden, A.A., Greiner, J. et al., Astrophys. J., 592, 1025

Maiolino, R., Marconi, A.& Oliva, E. 2001, Astron. Astrophys., 365, 37

Mathis, J.S., Rumple W. & Nordsieck K.H. 1977, Astrophys. J., 217, 425

Mathis, J.S. 1986, Astrophys. J., 308, 281

Perna, R., Lazzati, D. & Fiore, F. 2003, Astrophys. J., 585, 775

Ramirez-Ruiz, E., Threntham, N. & Blain, A.W. 2002, MNRAS, 329, 465

Reichart, D.E. 2001a, Astron. Astrophys. Suppl. Series, 198, 2708

Reichart, D.E. 2001b, Astrophys. J., submitted (astro-ph 0107546)

Reichart, D.E. & Price, P.A. 2002, Astrophys. J., 565, 174

Scoville, N.Z. 1992, in 'The Astronomy and Astrophysics Encyclopedia, ed. S.P.. Maran, page 374, Fig.1

Simon, V., Hudec, R., Pizzichini, G. & Masetti, N. 2001, Astron. Astrophys., 377, 450

Van de Hulst, H.C. 1957, in Light scattering by small particle, ed. Wiley & sons

Venemans, B.P. & Blain, A.W. 2001, MNRAS, 325, 1477

Vergani, S.D. 2002, laurea thesis

Waxman, E. & Draine, B.T. 2000, Astrophys. J., 537, 796

Weingarnter, J.C. & Draine, B.T. 2001, Astrophys. J., 548, 296

Zerbi, F.M., Chincarini, G., Ghisellini, G. et al. 2002, Astron. Nachr., 322, 275